American Mineralogist, Volume 92, pages 829–836, 2007

Order and miscibility in the otavite–magnesite solid solution

F.A. Bromiley,[1] T. Boffa Ballaran,[1,*] F. Langenhorst,[2] and F. Seifert[1]

[1]Bayerisches Geoinstitut, Universitaet Bayreuth, D-95440 Bayreuth, Germany
[2]Friedrich-Schiller-Universitaet Jena, Institut fuer Geowissenschaften, Burgweg 11, D-07749 Jena

Abstract

The effects of cation substitution and ordering in the otavite ($CdCO_3$)–magnesite ($MgCO_3$) solid solution have been investigated on samples synthesized at 1 GPa in the temperature range 500–800 °C for run durations up to 120 h. A complete, disordered solid solution, with $R\bar{3}c$ symmetry, was obtained at 800 °C, whereas Mg and Cd show partial ordering within the cadmium dolomite stability field, with $R\bar{3}$ symmetry, at intermediate compositions in the temperature range 500–650 °C. Rietveld refinements for X-ray diffraction data show that variation of the *a*-axis is linear as a function of composition, independent of the degree of order, whereas the *c*-axis shows a positive deviation from linearity as a function of composition, decreasing with increasing degree of order. Octahedral bond distances of the 800 °C series vary linearly with composition. Site occupancies were used to determine the long-range order parameter, *Q*, for samples with $R\bar{3}$ symmetry. Q^4 varies linearly as a function of temperature, suggesting a tricritical phase transition with a critical transition temperature T_c of 702(10) °C. EDX-TEM compositional microanalyses of samples within two-phase regions are in good agreement with Rietveld refinements, and allow better constraint of phase boundaries.

Keywords: X-ray powder diffraction, otavite–magnesite solid solution, carbonates, phase transition, cation ordering

Introduction

The magnesite ($MgCO_3$)–calcite ($CaCO_3$) join is by far the most studied among the carbonate systems, due to its geological importance. The magnesite and calcite end-members are rhombohedral with $R\bar{3}c$ symmetry. The hexagonal unit cell consists of layers of M^{2+} atoms alternating with layers of planar CO_3^{2-} groups along the **c** axis. The M^{2+} atoms are coordinated to 6 oxygen atoms, each belonging to different CO_3^{2-} groups, forming corner-shared octahedra. At intermediate compositions a lower symmetry phase (dolomite [$MgCa(CO_3)_2$], space group $R\bar{3}$) forms due to the ordering of Ca^{2+} and Mg^{2+} onto alternating octahedral layers and slight rotation of the CO_3^{2-} groups. The processes driving the order-disorder phase transition, and the effects of cation substitution, are important for elucidating the behavior of the system. However, unmixing and ordering processes are likely to occur during quenching of samples belonging to the magnesite-calcite join due to the high temperatures required for their syntheses and/or cation disorder, and the high critical temperatures of the two solvi. The study of an analog system can provide easier experimental conditions and thus better constraints on the results obtained. Dolomite-type compounds are also found in other carbonate systems, such as ankerite or ferroan dolomite [$Ca(Mg,Fe,Mn)(CO_3)_2$], kutnahorite [$CaMn(CO_3)_2$], minrecordite [$CaZn(CO_3)_2$], and cadmium dolomite [$CdMg(CO_3)_2$] (see reviews in Reeder 1983 and Goldsmith 1983). From these, however, only Cd-dolomite, although unknown in nature, can be readily synthesized both in the ordered and in the disordered state (Goldsmith 1972; Capobianco et al. 1987). $CaFe(CO_3)_2$ can be synthesized only as a disordered compound at relatively high CO_2 pressure, and it has been suggested that the ordered phase may be stable at temperatures lower than 450 °C (Davidson et al. 1993). Ordered kutnahorite and minrecordite occur in nature, but to date have not been successfully synthesized (Goldsmith 1983). Goldsmith and Northrop (1965) presented limited data on the solid solubility of $ZnCO_3$ in calcite, but minrecordite, $CaZn(CO_3)_2$, was not observed in those experiments given that natural minrecordite crystallizes at relatively low temperatures (Garavelli et al. 1982). On the other hand, phase relations in the otavite $CdCO_3$–magnesite $MgCO_3$ system seem to model those of the $CaCO_3$–$MgCO_3$ join at more accessible experimental temperatures (Goldsmith 1972). A complete disordered $R\bar{3}c$ solid solution exists at temperatures above 850 °C, whereas at intermediate compositions $Cd_xMg_{1-x}(CO_3)_2$ undergoes a reversible ordering transformation in the temperature range between 675 and 825 °C. The order-disorder phase transformation for a sample of 50:50 composition has been investigated in some detail by Capobianco et al. (1987) who found that the long-range order parameter changes from unity to zero in the temperature range between 600–850 °C. The phase diagram for this system obtained from first principle calculations (Burton and Van de Walle 2003) is in qualitative to semiquantitative agreement with the experiments. Also the two-phase region between $CdCO_3$ and Cd-dolomite has been calculated to be much smaller than observed experimentally

* E-mail: tiziana.boffa-ballaran@uni-bayreuth.de

0003-004X/07/0506–829$05.00/DOI: 10.2138/am.2007.2315

(Goldsmith 1972). The aim of this study is to characterize the mixing behavior of the otavite–magnesite solid solution, and to investigate the character of the order-disorder phase transition as a function of temperature and composition.

Experimental methods

Synthesis

$MgCO_3$ (Alfa Aesar, purity 99.996%) and $CdCO_3$ (Aldrich Chemicals, purity 99.999%) were mixed in appropriate amounts and homogenized in a piston cylinder apparatus at a pressure of 1 GPa with runs times of 1–120 h in a temperature range 500–800 °C. Silver oxalate, enclosed in Pt foil, was welded into a platinum capsule with the starting material, acting as an internal CO_2 source to prevent dissociation of carbonate material (Table 1). Experiments were quenched at run pressure by switching off the power, and temperatures below 100 °C were reached in less than 10 s.

X-ray powder diffraction

The run products were characterized by X-ray powder diffraction at room temperature using a Philips X'Pert Pro X-ray diffraction system operating in reflection mode, with Co$K\alpha_1$ (λ = 1.78897 Å) radiation selected with a focusing monochromator, a symmetrically cut curved Johansson $Ge_{(111)}$ crystal, and a Philips X'celerator detector. The $K\alpha_2$ line was reduced by the monochromator to <2% of the intensity of the $K\alpha_1$ line.

Samples, together with some Si (NBS standard material no. 640) as an internal standard, were examined by X-ray diffraction methods with diffractometer settings step size 0.02°, step time 1000 s, spinning platform rotation 1/s, and collection range 2θ = 20°–120°. Diffraction patterns were calibrated using the peak positions of the Si standard pattern and STOE Win XPOW (version 1.08, Stoe and Cie GmbH) software, then refined using a full pattern profile fitting (Rietveld analysis) with GSAS (Larson and Van Dreele 1994) and the Windows interface, EXPGUI (Toby 2001). Samples were refined in the rhombohedral system using the $R\bar{3}c$ space group for disordered samples and the $R\bar{3}$ space group for ordered carbonates. Atomic positions of magnesite (Oh et al. 1973), otavite (Borodin et al. 1979; Reeder 1983) and dolomite (Reeder and Wenk 1983) were used as starting parameters for the refinements of Mg-rich, Cd-rich, and ordered samples, respectively. The background function, scale factors, unit-cell parameters, atomic positional parameters, Gaussian and Lorentzian broadening coefficients of the pseudo-Voigt profile function and March-Dollase preferred orientation parameter (Dollase 1986; March 1932) were refined for all diffraction patterns. Soft restraints were used for the mean C-O bond lengths of the carbonate group that have been found to be very close to 1.28 Å for several carbonate phases, including magnesite and otavite (Zemann 1981). Cation site occupancies of Mg and Cd were refined only for the $R\bar{3}$ samples and were constrained to the nominal composition of the sample. Isotropic displacement parameters were refined during the last least-square cycles only for magnesite, for the $Mg_{0.9}Cd_{0.1}CO_3$ sample synthesized at 800 °C and for the ordered 50:50 sample synthesized at 600 °C for 96 h. The values so obtained were kept fixed during the Rietveld refinements of all other samples. This strategy was adopted due to large correlations observed between the isotropic temperature factors and the March-Dollase preferred orientation parameter for Cd-rich samples for which preferred orientation appears to be severe. The resulting Rietveld refinements obtained for the 800 °C magnesite and for the ordered 50:50 sample synthesized at 600 °C for 96 h are reported as an example in Figure 1. Unit-cell parameters, atomic positional parameters, octahedral mean bond distances, and site occupancies are reported in Tables 1–3.

Transmission electron microscopy (TEM)

Two two-phase samples ($Mg_{0.8}Cd_{0.2}CO_3$ and $Mg_{0.7}Cd_{0.3}CO_3$ synthesized at 600 °C, 3 h) and three samples showing broad diffraction peaks ($Mg_{0.6}Cd_{0.4}CO_3$ synthesized at 600 °C for 3 h, $Mg_{0.3}Cd_{0.7}CO_3$ synthesized at 500 °C for 24 h, and $Mg_{0.8}Cd_{0.2}CO_3$ synthesized at 800 °C for 1 h) were studied using a Philips CM20 Field Emission gun scanning transmission electron microscope (STEM), equipped with a Noran vantage energy dispersive X-ray (EDX) analyzer. For TEM study, sample powders were suspended in ethanol and then loaded onto holey carbon grids. The analytical TEM was then used for both conventional (bright-field and dark-field) imaging and electron diffraction as well as quantitative chemical analysis.

Selected area electron diffraction (SAED) experiments helped to distinguish between ordered and disordered domains that existed within the same sample. Due to the small grain size of synthesized samples (<1 μm), chemical compositions of coexisting phases could only be determined using EDX-TEM microanalysis. Since the EDX system was equipped with an ultra-thin window, light elements such as oxygen were measurable and analyses could be quantified on the basis of the principle of electroneutrality (Van Cappellen and Doukhan 1994; Langenhorst et al. 1995). Thereby the O*K* line served as a measure for the absorption correction. For the quantification of Mg and Cd contents we used the Mg*K* and Cd*L* lines, whereby the $k_{O/Cd}$ factor was calibrated using pure $CdCO_3$ as standard material. Since the TEM grid and samples were coated with carbon, the quantification procedure was run with a fixed carbon content of 20 at%. Analyses were acquired for sufficiently long live times to yield net counts between 20 000 to 80 000 Cts for O, Cd, and Mg. The statistical error of each individual analysis was thus reduced to 1–2%. The systematic error in *k* factors is estimated to be 2–3%. Table 4 gives compositional values averaged over at least 3 analyses.

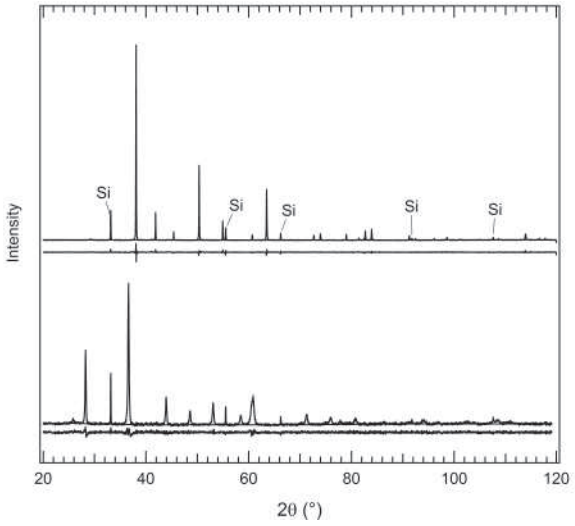

Figure 1. Examples of Rietveld refinements of the diffraction patterns obtained for magnesite synthesized at 800 °C for 1 h (top) and for $Mg_{0.5}Cd_{0.5}CO_3$ synthesized at 600 °C for 96 h (bottom).

Results

Powder X-ray diffraction

Most of the samples synthesized consisted of pure carbonate phases, although samples of composition $Mg_{0.9}Cd_{0.1}CO_3$ and $MgCO_3$ synthesized at 600 °C for 3 h did contain a very small amount (~2%) of brucite [$Mg(OH)_2$]. At 800 °C all samples have $R\bar{3}c$ symmetry. Samples synthesized at intermediate compositions (X_{Mg} between 0.4 and 0.6) and at 600 °C resulted in ordered carbonates with $R\bar{3}$ symmetry. Samples of composition $Mg_{0.7}Cd_{0.3}CO_3$ and $Mg_{0.8}Cd_{0.2}CO_3$ synthesized at 600 °C showed the presence of two carbonate phases of distinct composition and symmetry, whereas samples with the same composition but synthesized at 800 °C appear to consist of only one phase although they have very broad diffraction peaks. The Cd-rich samples showed only one phase to be present at all temperatures, although in the sample of composition $Mg_{0.3}Cd_{0.7}CO_3$ synthesized at 500 °C very broad diffraction peaks were observed.

Unit-cell parameters obtained for the 600 and 800 °C series are shown as a function of composition in Figure 2. For samples of composition $Mg_{0.7}Cd_{0.3}CO_3$ and $Mg_{0.8}Cd_{0.2}CO_3$ synthesized at 600 °C two values are reported, one for each of the two phases present in these run products. Note that the *a*-axis and the unit-

TABLE 1. Unit-cell parameters for all samples synthesized in the otavite–magnesite solid solution

Samples	X_{Mg}*	Space group	a (Å)	c (Å)	V (Å^3)
Samples synthesized at 500 °C and 1 GPa for 96 h					
$Mg_{0.3}Cd_{0.7}CO_3$	0.3†	$R\bar{3}c$	4.8422(7)	15.969(2)	324.26(9)
$Mg_{0.5}Cd_{0.5}CO_3$	0.5	$R\bar{3}$	4.7821(8)	15.697(1)	310.87(9)
Disordering at 600 °C of the 50:50 sample synthesized at 500 °C and 1 GPa for 96 h					
20 min	0.5	$R\bar{3}$	4.7822(9)	15.691(2)	310.77(9)
48 h	0.5	$R\bar{3}$	4.7819(9)	15.698(2)	310.86(9)
Samples synthesized at 600 °C and 1 GPa for 3 h					
$CdCO_3$	0.0	$R\bar{3}c$	4.9207(3)	16.2968(4)	341.73(5)
$Mg_{0.1}Cd_{0.9}CO_3$	0.1	$R\bar{3}c$	4.8950(2)	16.1938(4)	336.04(5)
$Mg_{0.2}Cd_{0.8}CO_3$	0.2	$R\bar{3}c$	4.8670(2)	16.0787(4)	329.85(5)
$Mg_{0.3}Cd_{0.7}CO_3$	0.3	$R3c$	4.8398(2)	15.9621(6)	323.80(5)
$Mg_{0.4}Cd_{0.6}CO_3$	0.4	$R\bar{3}$	4.8113(3)	15.8356(9)	317.46(7)
$Mg_{0.5}Cd_{0.5}CO_3$	0.5	$R\bar{3}$	4.7792(2)	15.6884(5)	310.32(5)
$Mg_{0.6}Cd_{0.4}CO_3$	0.6	$R\bar{3}$	4.7590(7)	15.5956(10)	305.90(8)
$Mg_{0.7}Cd_{0.3}CO_3$	‡,†	$R3$	4.7612(8)	15.603(3)	306.30(9)
		$R\bar{3}c$	4.659(1)	15.186(5)	285.4(2)
$Mg_{0.8}Cd_{0.2}CO_3$	‡,†	$R\bar{3}$	4.7589(8)	15.602(3)	306.01(9)
		$R\bar{3}c$	4.665(1)	15.187(4)	286.2(2)
$Mg_{0.9}Cd_{0.1}CO_3$	0.9†	$R3c$	4.6618(7)	15.1656(10)	285.43(7)
$MgCO_3$	1.0	$R\bar{3}c$	4.6338(3)	15.0192(4)	279.28(5)
Samples synthesized at 600 °C and 1 GPa for 19 h					
$Mg_{0.4}Cd_{0.6}CO_3$	0.4	$R\bar{3}$	4.8116(4)	15.8303(9)	317.39(7)
$Mg_{0.45}Cd_{0.55}CO_3$	0.45	$R\bar{3}$	4.7963(4)	15.7663(8)	314.10(6)
$Mg_{0.5}Cd_{0.5}CO_3$	0.5	$R\bar{3}$	4.7813(3)	15.7023(7)	310.88(5)
$Mg_{0.55}Cd_{0.45}CO_3$	0.55†	$R\bar{3}$	4.7752(8)	15.673(1)	309.5(1)
$Mg_{0.6}Cd_{0.4}CO_3$	0.6†	$R\bar{3}$	4.7632(9)	15.609(2)	306.7(2)
Sample synthesized at 600 °C and 1 GPa for 96 h					
$Mg_{0.5}Cd_{0.5}CO_3$	0.5	$R\bar{3}$	4.7818(5)	15.7028(7)	310.95(5)
Sample synthesized at 650 °C and 1 GPa for 120 h					
$Mg_{0.5}Cd_{0.5}CO_3$	0.5	$R\bar{3}$	4.7824(6)	15.7082(8)	311.13(8)
Sample synthesized at 700 °C and 1 GPa for 24 h					
$Mg_{0.5}Cd_{0.5}CO_3$	0.5	$R\bar{3}c$	4.7820(7)	15.7028(9)	310.97(9)
Samples synthesized at 800 °C and 1 GPa for 1 h					
$CdCO_3$	0.0	$R\bar{3}c$	4.9204(3)	16.2948(5)	341.65(7)
$Mg_{0.1}Cd_{0.9}CO_3$	0.1	$R\bar{3}c$	4.8934(3)	16.1892(5)	335.72(6)
$Mg_{0.2}Cd_{0.8}CO_3$	0.2	$R\bar{3}c$	4.8638(3)	16.0679(5)	329.19(6)
$Mg_{0.3}Cd_{0.7}CO_3$	0.3	$R\bar{3}c$	4.8341(5)	15.9434(9)	322.66(8)
$Mg_{0.4}Cd_{0.6}CO_3$	0.4	$R\bar{3}c$	4.8095(4)	15.8358(8)	317.23(6)
$Mg_{0.5}Cd_{0.5}CO_3$	0.5	$R\bar{3}c$	4.7788(4)	15.6968(8)	310.43(6)
$Mg_{0.6}Cd_{0.4}CO_3$	0.6	$R\bar{3}c$	4.7510(4)	15.5745(8)	304.45(6)
$Mg_{0.7}Cd_{0.3}CO_3$	0.7†	$R\bar{3}c$	4.7265(6)	15.4640(10)	299.18(10)
$Mg_{0.8}Cd_{0.2}CO_3$	0.8†	$R\bar{3}c$	4.6923(6)	15.3197(10)	292.17(10)
$Mg_{0.9}Cd_{0.1}CO_3$	0.9	$R\bar{3}c$	4.6638(4)	15.1720(5)	285.79(5)
$MgCO_3$	1.0	$R\bar{3}c$	4.6334(3)	15.0178(4)	279.21(5)

Notes: Standard deviations are in parentheses.
* Nominal compositions.
† Only unit-cell parameters have been refined.
‡ Two phases run products.

TABLE 2. Atomic positions of oxygen (x_O, y_O, z_O) and carbon (z_C)

X_{Mg}*	S.G.	x_O	y_O	z_O	z_C
Sample synthesized at 500 °C and 1 GPa for 96 h					
0.5†	$R\bar{3}$	0.252(2)	–0.026(2)	0.254(4)	0.245(4)
Disordering at 600 °C of the sample synthesized at 500 °C and 1 GPa for 96 h					
0.5† (20 min)	$R\bar{3}$	0.252(5)	–0.026(5)	0.249(8)	0.240(8)
0.5† (48 h)	$R\bar{3}$	0.252(5)	–0.026(5)	0.249(8)	0.239(8)
Samples synthesized at 600 °C and 1 GPa for 3 h					
0.0‡	$R\bar{3}c$	0.260(2)	0.0	0.25	0.25
0.1‡	$R\bar{3}c$	0.260(2)	0.0	0.25	0.25
0.2‡	$R\bar{3}c$	0.264(2)	0.0	0.25	0.25
0.3‡	$R\bar{3}c$	0.264(2)	0.0	0.25	0.25
0.4†	$R\bar{3}c$	0.251(2)	–0.024(2)	0.256(4)	0.246(4)
0.5†	$R\bar{3}$	0.252(2)	–0.025(2)	0.254(4)	0.244(4)
0.6†	$R\bar{3}$	0.254(3)	–0.025(3)	0.255(4)	0.247(4)
1.0#	$R\bar{3}c$	0.279(2)	0.0	0.25	0.25
Samples synthesized at 600 °C and 1 GPa for 19 h					
0.4†	$R\bar{3}$	0.252(2)	–0.025(2)	0.256(4)	0.249(4)
0.45†	$R\bar{3}$	0.252(2)	–0.025(2)	0.255(4)	0.246(4)
0.5†	$R\bar{3}$	0.252(4)	–0.026(4)	0.252(4)	0.244(3)
0.55†	$R\bar{3}$	0.252(5)	–0.026(5)	0.255(6)	0.244(6)
Sample synthesized at 600 °C and 1 GPa for 96 h					
0.5**	$R\bar{3}$	0.252(2)	–0.026(2)	0.252(3)	0.243(3)
Sample synthesized at 650 °C and 1 GPa for 120 h					
0.5†	$R\bar{3}$	0.254(2)	–0.023(2)	0.255(4)	0.249(4)
Sample synthesized at 700 °C and 1 GPa for 24 h					
0.5††	$R\bar{3}c$	0.265(2)	0.0	0.25	0.25
Samples synthesized at 800 °C and 1 GPa for 1 h					
0.0††	$R\bar{3}c$	0.260(2)	0.0	0.25	0.25
0.1††	$R\bar{3}c$	0.260(2)	0.0	0.25	0.25
0.2††	$R\bar{3}c$	0.264(2)	0.0	0.25	0.25
0.3††	$R\bar{3}c$	0.264(2)	0.0	0.25	0.25
0.4††	$R\bar{3}c$	0.266(2)	0.0	0.25	0.25
0.5††	$R\bar{3}c$	0.266(2)	0.0	0.25	0.25
0.6††	$R\bar{3}c$	0.268(2)	0.0	0.25	0.25
0.9§	$R\bar{3}c$	0.276(2)	0.0	0.25	0.25
1.0‖	$R\bar{3}c$	0.279(2)	0.0	0.25	0.25

Notes: For ordered samples, A (Cd-rich) and B (Mg-rich) sites are in Wyckoff positions 3a (0 0 0) and 3b (0 0 ½), respectively.
* Nominal compositions.
† For these samples the U_{iso} were fixed during the refinements to the values used for X_{Mg} = 0.5, 600 °C, 96 h.
‡ For these samples the U_{iso} were fixed during the refinements to the values used for X_{Mg} = 1, 600 °C, 3 h.
§ U_{iso} (x 100 Å^2): octahedral cations 2.9, carbon 3.6, oxygen 2.9.
‖ U_{iso} (x 100 Å^2): octahedral cations 2.8, carbon 2.2, oxygen 2.3.
U_{iso} (x 100 Å^2): octahedral cations 2.6, carbon 2.1, oxygen 2.1.
** U_{iso} (x 100 Å^2): octahedral cations 1.9, carbon 2.4, oxygen 1.4.
†† For these samples the U_{iso} were fixed during the refinements to the values used for X_{Mg} = 0.9, 800 °C, 1 h.

cell volume vary linearly as a function of composition, whereas the *c*-axis of the 800 °C series shows a small positive deviation from linearity. The curve reported in Figure 2 represents the best fit through the data of the 800 °C series with an equation similar to the symmetric expression for excess properties in regular solid solutions:

$$c = c_0 + c_1 X_{Mg} + c_2 X_{Mg}(1 - X_{Mg}) \quad (1)$$

where c_0, c_1, and c_2 are adjustable parameters.

The octahedral bond distances M-O of the $R\bar{3}c$ series synthesized at 800 °C vary linearly with composition (Fig. 3). Ordering of Mg and Cd onto alternating layers in the $R\bar{3}$ carbonate structure for samples at intermediate compositions synthesized at temperatures below 700 °C gives rise to two distinct cation sites A and B (with Cd preferentially occupying the A site), and hence to two distinct octahedral bond distances: A-O and B-O (Fig. 3). To accommodate the difference in bond lengths between the A and the B sites in ordered carbonates all the CO_3^{2-} groups within a given layer are uniformly rotated about the threefold axis relative to their position in the $R\bar{3}c$ structure. The angle of rotation, δ, defined as the angle between the C-O bond and the **a**-axis, is reported in Table 3. Moreover, for ordered carbonates, the C atom deviates slightly from the plane defined by the O atoms, so that the oxygen-carbon-oxygen bond angle, O-C-O, deviates from the 120° value of samples with $R\bar{3}c$ symmetry (Table 3). The same phenomenon has been observed for ordered (Ca,Mg)-dolomites (Reeder and Wenk 1983) and it has been ascribed to the difference in charge density between the M^{2+} atoms ordered

TABLE 3. Octahedral bond distances (Å), O-C-O and δ angles (°), Cd and Mg site occupancies, and order parameter *Q*

X_{Mg}*	A-O	B-O	M-O	O-C-O	δ	Cd_A	Mg_B	Q
Sample synthesized at 500 °C and 1 GPa for 96 h								
0.5	2.239(11)	2.185(12)	2.212	118.7(5)	7.7(5)	0.686(8)	0.686(8)	0.346
Disordering at 600 °C of the sample synthesized at 500 °C and 1 GPa for 96 h								
0.5(20 min)	2.29(2)	2.13(2)	2.21	118.8(9)	8.0(5)	0.645(8)	0.645(8)	0.290
0.5(48 h)	2.28(2)	2.14(2)	2.21	118.5(9)	8.7(5)	0.629(8)	0.629(8)	0.258
Samples synthesized at 600 °C and 1 GPa for 3 h								
0.0			2.293(6)					
0.1			2.280(6)					
0.2			2.256(6)					
0.3			2.242(6)					
0.4	2.240(9)	2.228(10)	2.234	118.4(5)	8.7(5)	0.718(8)	0.518(8)	0.246
0.5	2.238(10)	2.185(11)	2.211	118.5(5)	8.6(5)	0.595(8)	0.595(8)	0.190
0.6	2.211(9)	2.183(10)	2.197	118.9(5)	7.6(5)	0.488(8)	0.688(8)	0.183
1.0			2.099(6)					
Samples synthesized at 600 °C and 1 GPa for 19 h								
0.4	2.241(13)	2.220(16)	2.230	119.4(9)	6.4(5)	0.744(9)	0.544(9) esds?	0.300
0.45	2.239(9)	2.206(11)	2.222	118.7(7)	8.1(5)	0.703(9)	0.603(9)	0.309
0.5	2.259(10)	2.162(14)	2.214	119.0(9)	7.5(5)	0.634(8)	0.634(8)	0.268
0.55	2.231(13)	2.189(15)	2.210	118.1(9)	9(1)	0.552(10)	0.652(10)	0.206
Sample synthesized at 600 °C and 1 GPa for 96 h								
0.5	2.263(9)	2.158(10)	2.194	118.9(6)	7.8(5)	0.638(5)	0.638(5)	0.276
Sample synthesized at 650 °C and 1 GPa for 120 h								
0.5	2.222(9)	2.200(10)	2.211	119.3(7)	6.4(5)	0.629(8)	0.629(8)	0.258
Sample synthesized at 700 °C and 1 GPa for 24 h								
0.5			2.208(6)					
Samples synthesized at 800 °C and 1 GPa for 1 h								
0.0			2.293(6)					
0.1			2.278(7)					
0.2			2.255(10)					
0.3			2.240(6)					
0.4			2.221(6)					
0.5			2.206(6)					
0.6			2.187(6)					
0.9			2.122(6)					
1.0			2.099(6)					

Notes: Samples with $R\bar{3}c$ symmetry have only one octahedral bond distance, and random occupancy of Mg and Cd onto the octahedral sites, moreover the O-C-O and δ angles are constrained by symmetry to be 120° and 0°, respectively. For samples with $R\bar{3}$ symmetry, M-O is the mean bond distance of the octahedral A-O and B-O distances.
* Nominal compositions.

into alternating layers (Lippmann 1973).

The convergent long-range cation ordering in Cd-dolomite can be described with a Landau expansion of the order parameter *Q* defined in terms of cation occupancies of Mg and Cd on the octahedral sites with an equation similar to that used to describe cation ordering in omphacites (Boffa Ballaran et al. 1998; Carpenter et al. 1990):

$$Q = \left[\frac{Cd_{M2} - Cd_{M1}}{\sum Cd} + \frac{Mg_{M1}\text{-}Mg_{M2}}{\sum Mg}\right] \times 0.5 \quad (2)$$

where the differences between the occupancies of the Mg and Cd on the two sites are scaled with respect to the total amount of Cd and Mg, so the expression can also be used for compositions other than $Mg_{0.5}Cd_{0.5}CO_3$. The value of *Q* varies between zero (complete disorder) and one (complete order). The resulting long-range order parameters are reported in Table 3 for all ordered samples and show that only partial order has been achieved. In the simplest case the variation of *Q* with temperature may be expressed as:

$$Q = \left(1 - \frac{T}{T_c}\right)^{\beta} \quad \text{for } T < T_c \quad (3)$$

TABLE 4. Chemical compositions from EDX-TEM microanalysis

Samples	X_{Mg}*	X_{Cd}*	X_{Mg}†	X_{Cd}†
Sample synthesized at 500 °C and 1 GPa for 96 h				
$Mg_{0.3}Cd_{0.7}CO_3$	0.27	0.73	0.33	0.67
Samples synthesized at 600 °C and 1 GPa for 3 h				
$Mg_{0.6}Cd_{0.4}CO_3$	0.54	0.46		
$Mg_{0.7}Cd_{0.3}CO_3$	0.86	0.14	0.59	0.41
$Mg_{0.8}Cd_{0.2}CO_3$	0.90	0.10	0.54	0.46
Sample synthesized at 800 °C and 1 GPa for 1 h				
$Mg_{0.8}Cd_{0.2}CO_3$	0.81	0.19		

*,† Mg and Cd content (apfu) of the carbonate phases present in the synthesis products. As indicated, three of these products resulted in two-phases mixture.

where T_c is the transition temperature of the order-disorder process and β = 0.5 for a second-order transformation and β = 0.25 for a tricritical transition (Putnis 1992). In the case of Cd-dolomite, the data are consistent with a linear behavior of Q^4 as a function of temperature (Fig. 4) indicative of a tricritical order-disorder phase transition. The linear fit through the data gives a critical temperature, T_c, for the order-disorder phase transition

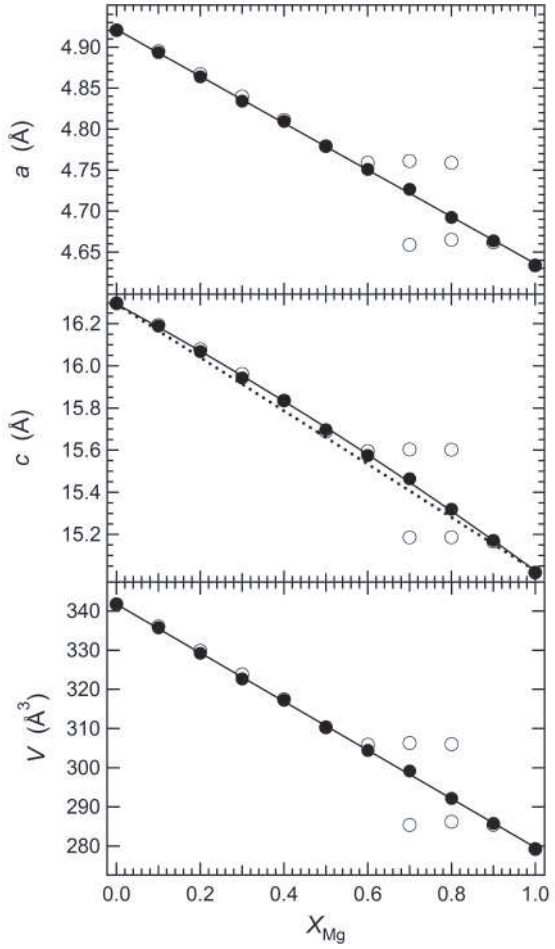

FIGURE 2. Unit-cell parameters as function of composition. Symbols: open circles = samples synthesized at 600 °C for 3 h, solid circles = samples synthesized at 800 °C for 1 h. The solid lines are the linear fits through the 800 °C data of the *a*-axis $a = 4.922(1) - 0.286(2)X_{Mg}$ and of the unit-cell volume $V = 341.7(2) - 62.1(4)X_{Mg}$. The solid curve represents the symmetric fit of the 800 °C *c*-axis data using Equation 1: $c = 16.293(7) - 1.265(9)X_{Mg} + 0.19(3)X_{Mg}(1 - X_{Mg})$. The dashed straight line connects the unit-cell *c*-axis values of the end-members.

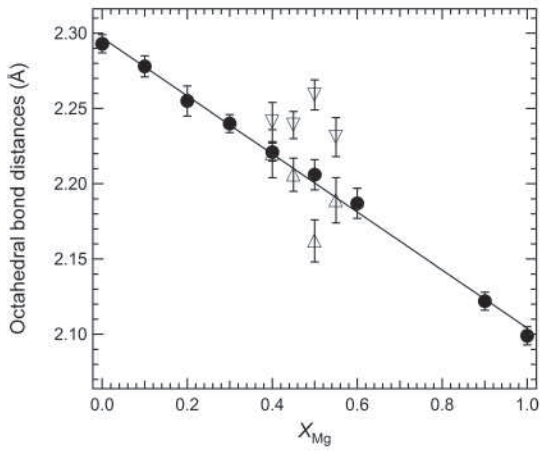

FIGURE 3. Octahedral bond distances along the otavite–magnesite join. Filled circles = samples synthesized at 800 °C; open triangles = ordered samples synthesized at 600 °C for 19 h.

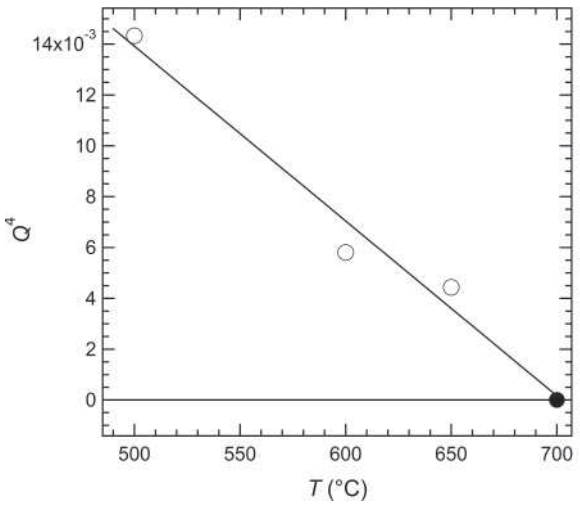

FIGURE 4. Variation of Q^4 for $Mg_{0.5}Cd_{0.5}CO_3$ samples synthesized at different temperatures. The solid line is a linear fit through the data: $Q^4 = 0.048(8) - 6(1) \times 10^{-5}T$. Open circles are samples with $R\bar{3}$ structure. Solid circle is for sample with $R\bar{3}c$ structure.

of 702 °C with an estimated uncertainty of ~10 °C.

From our data it is difficult to evaluate the effect of changing composition on the order-disorder transformation. The $Mg_{0.4}Cd_{0.6}CO_3$ and $Mg_{0.45}Cd_{0.55}CO_3$ samples synthesized at 600 °C for 19 h show higher long-range order parameters Q than the $Mg_{0.5}Cd_{0.5}CO_3$ sample. The octahedral bond distances of the same samples appear to behave more consistently, therefore we could express the order parameter in terms of this structural feature with an expression similar to that used by Carpenter et al. (1990) to describe cation ordering in omphacites:

$$Q = C\frac{(A-O)-(B-O)}{\frac{1}{2}\left[(A-O)+(B-O)\right]} \quad (4)$$

where C is a constant if we assume a linear relationship between the cation-oxygen bond length and the site occupancies. The variations with composition of Q, Q^2, and Q^4 defined in terms of octahedral bond lengths are shown in Figure 5. With the present data it is difficult to discriminate between a second order and a tricritical transition (Carpenter et al. 1990) with changing composition, but the data in Figure 5 emphasize a minor asymmetry with respect to ordering relative to the $X_{Mg} = 0.5$ composition.

The occupancies of the cation sites for samples with $R\bar{3}$ symmetry were also used to investigate the kinetics of the ordering reaction, as well as its reversibility. The variation with time of the Mg occupancy on the B site for samples of composition $Mg_{0.5}Cd_{0.5}CO_3$ annealed at 600 °C is shown in Figure 6. The solid curve represents experiments in which samples were ordered from a completely disordered state (i.e., synthesized from a mixture of the end-members $CdCO_3$ and $MgCO_3$). From this curve it is possible to estimate that the ordering reaction reached equilibrium at approximately 10 h. The dashed curve shows disordering experiments to ascertain the equilibrium value. The

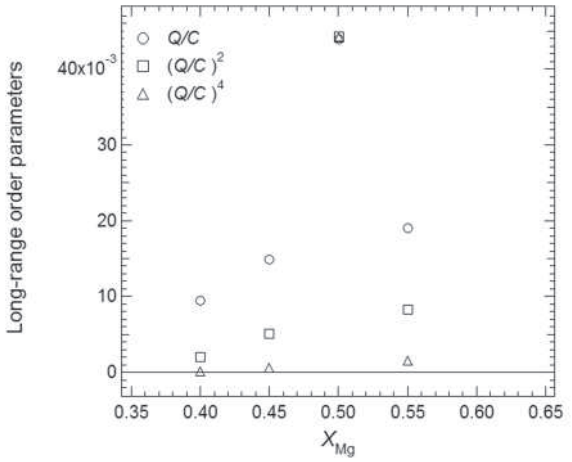

FIGURE 5. Variations of Q, Q^2, and Q^4 with composition as determined from octahedral bond distances (Eq. 4) for samples synthesized at 600 °C for 19 h.

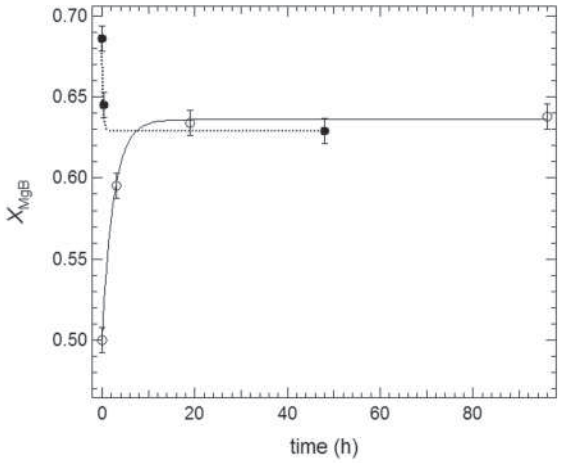

FIGURE 6. Variation of the Mg occupancy at the B site as a function of time. Open circles are ordering experiments conducted at 600 °C and 1 GPa using a 50:50 mixture of $CdCO_3$ and $MgCO_3$ end-members. Filled circles are disordering experiments conducted at 600 °C and 1 GPa using the $Mg_{0.5}Cd_{0.5}CO_3$ dolomite synthesized at 500 °C for 96 h as starting material.

most ordered sample, synthesized at 500 °C for 96 h, was used as a starting material in runs at 600 °C for durations of 20 min and 48 h. It appears that the disordering process reached equilibrium faster than the ordering process, which, in any case, shows that the equilibrium value at this temperature is tightly constrained by the disordering experiments.

Transmission electron microscopy

The sample of composition $Mg_{0.3}Cd_{0.7}CO_3$ synthesized at 500 °C for 24 h showed broad X-ray diffraction peaks and, according to the analysis with EDX, exhibits a small, but clear, difference in composition on the order of 5 mol% between the crystals analyzed (Table 4). Both samples of composition $Mg_{0.7}Cd_{0.3}CO_3$ and $Mg_{0.8}Cd_{0.2}CO_3$ synthesized at 600 °C for 3 h resulted in a mixture of two carbonate phases, one richer in Cd and with characteristic reflections due to Mg/Cd ordering on the octahedral sites and one richer in Mg and clearly disordered. Both samples displayed a difference in grain size according to the composition of the grain. Ordered crystals with $R\bar{3}$ symmetry were found to be in the order of ten times larger than those that were disordered ($R\bar{3}c$ symmetry). The samples of compositions $Mg_{0.8}Cd_{0.2}CO_3$ synthesized at 800 °C for 1 h and $Mg_{0.6}Cd_{0.4}CO_3$ synthesized at 600 °C for 3 h displayed very broad X-ray diffraction peaks, suggesting some degree of unmixing. However, this was not seen in the EDX analyses.

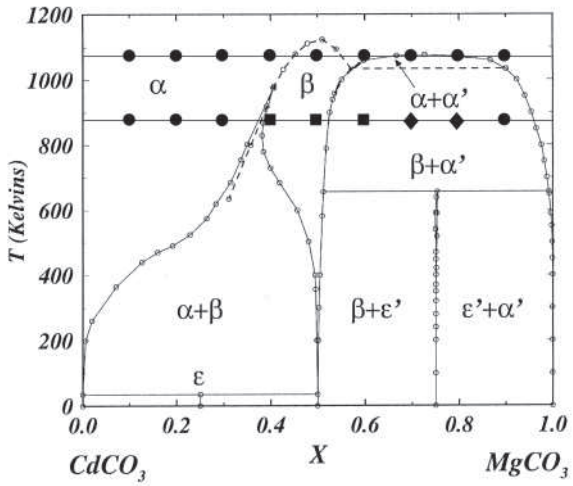

FIGURE 7. Experimental results of this study superimposed on the calculated phase diagram for the $CdCO_3$-$MgCO_3$ system reproduced from Figure 5 in Burton and Van de Walle (2003). Filled circles = $R\bar{3}c$ carbonate, filled squares = $R\bar{3}$ ordered Cd-dolomite samples; filled diamonds = two phase products.

DISCUSSION

Phase relations

Comparison of the Burton and Van de Walle (2003) study with results from this study are shown in Figure 7. In contrast to Goldsmith (1972), who observed a miscibility gap in the cadmium-rich half of the phase diagram at temperatures of ~650 °C, the study by Burton and Van de Walle (2003) shows a very narrow miscibility gap there, which is stable only up to ~600 °C. Cd-rich samples synthesized in this study consist of a single carbonate phase, in good agreement with the phase diagram proposed by Burton and Van de Walle (2003). Only the sample of composition $Mg_{0.3}Cd_{0.7}CO_3$ synthesized at 500 °C for this study consists of two carbonate phases having slightly different compositions, as obtained by means of EDX-TEM microanalysis. This sample lies close to the solvus of the miscibility gap calculated by Burton and Van de Walle (2003) (Fig. 7).

The main discrepancy between the data obtained here and the results of Goldsmith (1972), Capobianco et al. (1987), and Burton and Van de Walle (2003) is the compositional range over which the cadmium dolomite phase is stable. Goldsmith (1972) and Capobianco et al. (1987) show a very narrow stability field for Cd-dolomite between compositions $Mg_{0.45}Cd_{0.55}CO_3$ and $Mg_{0.55}Cd_{0.45}CO_3$ at 600 °C. The study by Burton and Van de

Walle (2003) gives phase boundaries for the ordered phase at a composition of $Mg_{0.4}Cd_{0.6}CO_3$, and in the magnesium-rich half of the phase diagram (Fig. 7), very close to the $Mg_{0.5}Cd_{0.5}CO_3$ composition. In contrast, the experimental results from this study show a larger stability field for the cadmium dolomite phase ($Mg_{0.4}Cd_{0.6}CO_3$-$Mg_{0.6}Cd_{0.4}CO_3$) at 600 °C from Rietveld refinements. However, whereas samples $Mg_{0.4}Cd_{0.6}CO_3$ and $Mg_{0.45}Cd_{0.55}CO_3$ have relatively sharp diffraction profiles, $Mg_{0.55}Cd_{0.45}CO_3$ and $Mg_{0.6}Cd_{0.4}CO_3$ have very broad diffraction patterns, suggesting asymmetric ordering behavior about the $Mg_{0.5}Cd_{0.5}CO_3$ composition. Quantification of the degree of asymmetry is difficult as structural values obtained from Rietveld refinements for sample $Mg_{0.55}Cd_{0.45}CO_3$ have very large uncertainties (Tables 2 and 3). Sample $Mg_{0.6}Cd_{0.4}CO_3$ proved even more problematic, and hence it was not possible to perform a Rietveld refinement for this sample. Results obtained from EDX analyses are in good agreement with Rietveld refinements, within error (Table 4). Compositional microanalysis suggests that at 600 °C the $R\bar{3}$ stability field exists over the compositional range $Mg_{0.45}Cd_{0.55}CO_3$-$Mg_{0.55}Cd_{0.45}CO_3$, being more consistent with previous studies. In the present study we obtained Cd-dolomite at much lower temperatures (~700 °C) then previously reported (Goldsmith 1972; Capobianco et al. 1987).

Cation substitution and ordering

The unit-cell parameters, oxygen coordinates, and M-O bond distances obtained in this study for the end-members are in good agreement with the values reported by Borodin et al. (1979), Effenberger et al. (1981), and Oh et al. (1973) from refinements of single-crystal data.

Variations of unit-cell parameters as a function of composition, similar to those observed in this study, i.e., a linear variation for the *a*-axis and a positive deviation from linearity for the *c*-axis, have also been observed for the $CaCO_3$-$CdCO_3$ solid solution, which is complete, as in our otavite-magnesite samples synthesized at 800 °C (Borodin et al. 1979; Chang and Brice 1971). However, the $CaCO_3$-$CdCO_3$ solid solution does not present an ordered phase at intermediate compositions at any temperature. In the otavite-magnesite join ordered Cd-dolomite samples have smaller *c*-axis values than the completely disordered samples with the same composition (Fig. 2). This trend has also been observed by Goldsmith (1972). Assuming that the *c*-axis values of completely ordered samples would lie on a straight line between the end-members, so displaying ideal behavior, one can calculate the strain associated with the order-disorder transformation defined as $\varepsilon = (c_{dis} - c_{ord})/c_{ord}$, where c_{dis} is the *c*-axis value calculated with Equation 1 for a sample of 50:50 composition and c_{ord} is the *c*-axis value obtained for the same composition from a straight line through the end-members. Therefore, the maximum strain calculated is $\varepsilon = 0.003$. For (Ca,Mg)-dolomites, Reeder and Wenk (1983) estimate that the Δc value between a completely ordered and a completely disordered (Ca,Mg)-dolomite is $\Delta c = 0.07$ Å, which corresponds to a strain of $\varepsilon = 0.004$ associated with the order-disorder transition.

Within the limited precision of the Rietveld refinements, octahedral bond distances vary linearly with composition (Fig. 3) for samples synthesized at 800 °C. This behavior supports the suggestion that for calcite-otavite and calcite-magnesite, octahedral bond distances follow a linear trend, although such suggestion was based only on the refinements of one Cd-calcite (Borodin et al. 1979) and three Mg-calcites samples (Althoff 1977; Paquette and Reeder 1990).

It is more difficult to evaluate the influence of cation ordering on the CO_3^{2-} groups. In ideal (Ca,Mg)-dolomite (i.e., totally ordered), charge densities of Ca layers differ significantly from those of adjacent Mg layers, so that oxygen atoms assume a position closer to Mg than Ca, with the result that the CO_3^{2-} groups are uniformly rotated about the threefold axis and that the carbon atoms are forced out of the plane of the oxygen atoms. The C-O bond in ideal (Ca,Mg)-dolomite is misaligned by ~6.6° from the **a**-axis. The net effect of increasing disorder is to decrease this angle of rotation, δ, toward zero (Reeder and Wenk 1983). Although the Cd-dolomite samples synthesized in this study are only partially ordered, their δ angles have values similar to those of completely ordered (Ca,Mg)-dolomites, moreover there is no clear trend as a function of decreasing order. Similarly, no clear trend is defined by the displacement of the carbon atoms along **c**, or the O-C-O angles, which deviate from 120° for ordered dolomites.

The most precise determination of the order parameter in this study is by means of the Rietveld technique, and it clearly demonstrates tricritical behavior (Fig. 4). This is possibly true for dolomite structures in general. If the order parameter variation of the disordering experiment of (Ca,Mg)-dolomite reported by Antao et al. (2004) is analyzed using a Landau expansion instead of the generalized Bragg-William model used by the authors, tricritical behavior is also found. It appears, therefore, that the order-disorder transition in dolomite is driven by a cooperative behavior of the divalent cations in the octahedral sites and the CO_3^{2-} groups.

Acknowledgments

This work has been financed by the Sofja Kovalevskaja Award to T. Boffa Ballaran. Geoffrey Bromiley assisted with the piston-cylinder syntheses. The authors also wish to thank J. Zemann and an anonymous referee for reviewing the manuscript.

References cited

Althoff, P.L. (1977) Structural refinements of dolomite and a magnesian calcite and implications for dolomite formation in the marine environment. American Mineralogist, 62, 772–783.

Antao, S.M., Mulder, W.H., Hassan, I., Crichton, W.A., and Parise, J.B. (2004) Cation disorder in dolomite, $CaMg(CO_3)_2$, and its influence on the aragonite + magnesite ↔ dolomite reaction boundary. American Mineralogist, 89, 1142–1147.

Boffa Ballaran, T., Carpenter, M.A., Chiara Domeneghetti, M., and Tazzoli, V. (1998) Structural mechanisms of solid solution and cation ordering in augite-jadeite pyroxenes: I. A macroscopic perspective. American Mineralogist, 83, 419–433.

Borodin, V.L., Lyntin, V.I., Ilyukhin, V.V., and Belov, N.V. (1979) Calcite-otavite isomorphous series. Doklady Akademii Nauk SSSR, 245, 1099–1101.

Burton, B.P. and Van de Walle, A. (2003) First-principles-based calculations of the $CaCO_3$-$MgCO_3$ and $CdCO_3$-$MgCO_3$ subsolidus phase diagrams. Physics and Chemistry of Minerals, 30, 88–97.

Capobianco, C., Burton, B.P., Davidson, P.M., and Navrotsky, A. (1987) Structural and calorimetric studies of order-disorder in $CdMg(CO_3)_2$. Journal of Solid State Chemistry, 71, 214–223.

Carpenter, M.A., Domeneghetti, M.C., and Tazzoli, V. (1990) Application of Landau theory to cation ordering in omphacite II: Kinetic behavior. European Journal of Mineralogy, 2, 19–28.

Chang, L.L.Y. and Brice, W.R. (1971) Subsolidus phase relations in the system calcium carbonate-cadmium carbonate. American Mineralogist, 56, 338–341.

Davidson, P.M., Symmes, G.H., Cohen, B.A., Reeder, R.J., and Lindsley, D.H. (1993) Synthesis of the new compound $CaFe(CO_3)_2$ and experimental

constraints on the $(Ca,Fe)CO_3$ join. Geochimica et Cosmochimica Acta, 57, 5105–5109.
Dollase, W.A. (1986) Correction of intensities for preferred orientation in powder diffractometry-application of the March model. Journal of Applied Crystallography, 19, 267–272.
Effenberger, H., Mereiter, K., and Zemann, J. (1981) Crystal structure refinements of magnesite, calcite, rhodochrosite, siderite, smithsonite and dolomite, with discussion of some aspects of the stereochemistry of calcite-type carbonates. Zeitschrift für Kristallographie, 156, 233–243.
Garavelli, C.G., Vurro, F., and Fioravanti, G.C. (1982) Minrecordite, a new mineral from Tsumeb. Mineralogical Record, 13, 131–136.
Goldsmith, J.R. (1972) Cadmium dolomite and the system $CdCO_3$-$MgCO_3$. Journal of Geology, 80, 617–626.
——— (1983) Phase relations of rhombohedral carbonates. In R.J. Reeder, Ed. Carbonates: Mineralogy and Chemistry, 11, p. 49–76. Reviews in Mineralogy, Mineralogical Society of America, Chantilly, Virginia.
Goldsmith, J.R. and Northrop, D. (1965) Subsolidus phase relations in the system $CaCO_3$-$MgCO_3$-$CoCO_3$ and $CaCO_3$-$MgCO_3$-$NiCO_3$. Journal of Geology, 73, 817–829.
Langenhorst, F., Joreau, P. and Doukhan, J.C. (1995) Thermal and shock metamorphism of the Tenham chondrite: A TEM examination. Geochimica et Cosmochimica Acta, 59, 1835–1845.
Larson, A. and Van Dreele, R.B. (1994) GSAS General Structure Analysis System. Los Alamos National Laboratory, New Mexico.
Lippmann, F. (1973) Sedimentary Carbonate Minerals. Springer-Verlag, New York.
March, A. (1932) Mathematical theory on regulation according to the particle shape and affine deformation. Zeitschrift für Kristallographie, 81, 285–297.
Oh, K.D., Morikawa, H., Iwai, S.i., and Aoki, H. (1973) The crystal structure of magnesite. American Mineralogist, 58, 1029–1033.
Paquette, J. and Reeder, R.J. (1990) Single-crystal X-ray structure refinements of two biogenic magnesian calcite crystals. American Mineralogist, 75, 1151–1158.
Putnis, A. (1992) Introduction to Mineral Sciences. Cambridge University Press, U.K.
Reeder, R.J. (1983) Crystal chemistry of the rhombohedral carbonates. In R.J. Reeder, Ed. Carbonates: Mineralogy and Chemistry, 11, p. 1–47. Reviews in Mineralogy, Mineralogical Society of America, Chantilly, Virginia.
Reeder, R.J. and Wenk, H.-R. (1983) Structure refinements of some thermally disordered dolomites. American Mineralogist, 68, 769–776.
Toby, B.H. (2001) EXPGUI, a graphical user interface for GSAS. Journal of Applied Crystallography, 34, 210–213.
Van Cappellen, E. and Doukhan, J.C. (1994) Quantitative X-ray microanalysis of ionic compounds. Ultramicroscopy, 53, 343–349.
Zemann, J. (1981) Zur Stereochemie der Karbonate. Fortschritte der Mineralogie, 59, 95–116.

Manuscript received May 19, 2006
Manuscript accepted January 10, 2007
Manuscript handled by Eugen Libowitzky